Numerical simulation of coronary blood flow in idealized composite arterial coronary grafts

Argyris K. Politis, George P. Stavropoulos, Nicholas S. Vlachos and Nicholas C. Markatos

Abstract—**In Composite Arterial Coronary Grafts (CACGs), local blood dynamics play a major role on the localization of Coronary Artery Disease (CAD). However, the underlying mechanisms involving to the initiation and progression of atherosclerosis are not well determined in relevant literature. Coronary arterial geometries, surgically constructed after bypass grafting, may remarkably alter the local haemodynamics leading to undesirable complications such as arterial restenosis and heart attack. In this study, a mathematical model using Computational Fluid Dynamics (CFD) is rigorously implemented to examine the main transport parameters influence the blood flow within different geometric configurations of CACGs. The computational results focus on local haemodynamics, such as velocity flow fields, spatial and temporal variations of WSSs which are highly correlated with atherogenetic factors. Prominent variations on the velocity and WSS distributions are observed for the various CACGs, particularly at the anastomotic sites.**

I. Introduction

CORONARY bypass grafting is widely applied in the modern practice of cardiac surgery aiming at rehabilitating pathological conduits. Moreover, it is well established that local blood dynamics play an important role in the development and progression of coronary pathologies. However, the exact mechanisms in which endothelium responds to flow alterations driven by unsteadiness, anatomy and level of pathology have not yet been well-elucidated. The numerical investigation of blood flow within coronary arterial conduits has gained a lot of research interest, since it has been proved that CFD techniques may provide a powerful tool in assisting surgical planning. The main goal of this paper is to provide a robust numerical analysis tool, based on CFD methods in order to assist non-invasive diagnostic techniques and to predict the main hemodynamic parameters associated with the occurrence of CAD.

Manuscript received July 5, 2008.

A. K. Politis is with the National Technical University of Athens, 9 Heroon Polytechneiou St., 15780, Athens, Greece (corresponding author: phone: +30 210 772 3147; fax: +30 210-772 3228; e-mail: apolit_5@yahoo.gr)

G. P. Stavropoulos was with Henri Dunant Hospital, 107 Mesogion St., Athens, Greece. He is now with the Department of Cardiac Surgery, Hippokration Hospital, 114 Vas. Sofias St., 11527, Athens, Greece (e-mail: gstavrop@yahoo.com).

N. S. Vlachos is with the Department of Mechanical & Industrial Engineering, University of Thessaly, Volos, Thessaly, Greece (e-mail: vlachos@mie.uth.gr).

N. C. Markatos is with the National Technical University of Athens, 9 Heroon Polytechneiou St., 15780, Athens, Greece (e-mail: n.markatos@ ntua.gr).

In bypass grafting, the most powerful predictor of good long term results, as far as morbidity and mortality are concerned, in the surgical treatment of CAD is to anastomose the Left Internal Thoracic Artery (LITA) to the Left Anterior Descending (LAD) artery [1]. The current trend in surgical treatment is to use exclusively arterial grafts, even in the non-LAD territory. Thus, the concept of Total Arterial Revascularization (TAR) is well established in the routine treatment of patients with good life expectancy [2]. Due to the lack of sufficient length of pedicled arterial grafts to by-pass the target lesions of the native coronary vessels, it is obligatory to construct composite arterial grafts according to the anatomy of the native coronary network. These composite grafts consist mainly of different segments of internal thoracic and radial arteries [3]. These grafts are commonly conjugated to function either in parallel as Y and T grafts or in series as a sequential graft. The above functional classification of Composite Arterial Coronary Grafts (CACGs) is based on the arrangement of flow resistances due to the arterial bifurcations. In some cases, a more complex composite graft has been used to revascularize more than one distal vessels, namely a Π-graft [4] (Fig. 1), which practically is a double T-graft.

Even though CACGs are routinely used in cardiac surgery, it is still under investigation whether or not the transport of oxygen via blood that systematically circulates in those grafts can adequately meet the metabolic demands of the native myocardial function, especially under different loading conditions of the heart (coronary flow reserve). According to a positron emission tomography (PET) study carried out by Sakaguchi et al. (2002) [5] concerning the coronary flow reserve of composite grafts in a set of post-operative coronary by-pass patients, the myocardial blood flow failed to meet the increased oxygen demands during treadmill test. Therefore, it is of paramount importance to conduct in vitro investigation of coronary haemodynamics for different geometric configurations used in surgical treatment of CAD, in order to gain better insight into this subject. This investigation is missing in the current literature.

The impact of geometry on both single-and multi-branched coronaries is fully investigated herein, in terms of flow rate ratios, velocity profiles and Wall Shear Stress (WSS) distributions. The numerical results aim at correlating the complexity of CACGs with local haemodynamics numerically predicted by CFD simulations. Moreover, the numerical prediction of pathological cases, that includes different degrees of native artery severity stenoses are incorporated in this study. The performed computations will be validated with flow measurements conducted on an

experimental rig that simulates the blood flow within different configurations of CACGs.

II. MATERIALS & METHODS

A. Computational Geometry

Figure 1 shows the geometrical configurations for different CACGs simulated with a CFD code. The composite graft geometries are developed as an analytical intersection of two (T- and Y-grafts) or three cylinders (Sequential and Π-graft) with circular cross sections [6]. The computational grids were generated by multi-block approach as described by [7]. The meshes employed herein are constructed in Body Fitted Coordinates (BFC) with a non-uniform distribution of control volumes, especially in the vicinity of anastomoses in

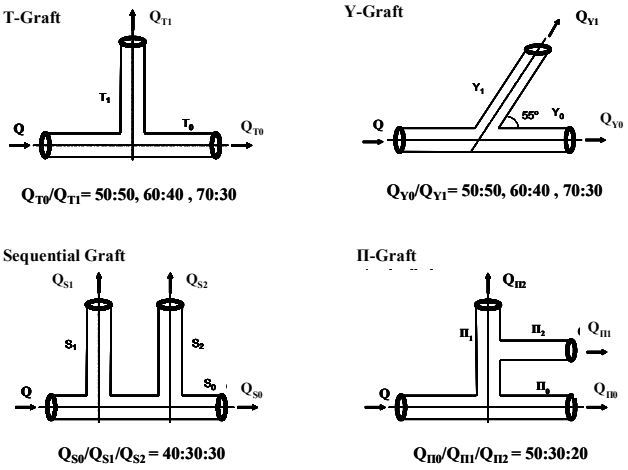

Figure 1: Geometrical configurations of idealized CACGs. A known distribution of flow rates is imposed at outlets. The outflow rates are subscripted with Q.

order to resolve steep gradients of transport quantities.

In Table 1 the rheological properties used for computer-based modeling as well as the geometric characteristics of computational domains are provided. The host coronary artery diameter is D_1 with a total length of $30D_1$. The lengths of first side branches (Graft-1) are $20D_1$ in all cases while the second side branches (Graft-2) are $20D_1$ for Sequential and 15 D_1 for Π-graft. The coronary artery dimensions were consistent with values reported by Calafiore et al., 1994 [4]. Furthermore, as reported by Liepsch, 2002 [8] the graft diameters must be equal or less than the host artery.

B. Mathematical Modeling

The equations govern the three-dimensional, unsteady flow are the mass and momentum conservations as shown in equations (1) and (2):

$$\rho\left(\frac{\partial \vec{u}}{\partial t}+\vec{u}\cdot\vec{\nabla}\vec{u}\right)=-\vec{\nabla}p+\mu\,\vec{\nabla}^2\vec{u} \qquad (1)$$

$$\frac{\partial \rho}{\partial t}+\nabla\cdot\left(\rho\vec{u}\right)=0 \qquad (2)$$

where ρ is the fluid density, $\vec{u}$ the velocity vector, p the pressure. The terms on the left hand side of equation (1) denote the substantive derivative for the local and convective acceleration. The right hand side of equation (1) is consisted of the pressure gradient and the viscous term (Laplace equation). In equation (2) the unsteady, three dimensional mass conservation or continuity equations are depicted.

The complex geometries presented in this study are written and subsequently solved in Generalized Curvilinear Coordinates (GCC). The three-dimensional Navier-Stokes

TABLE 1
DIMENSIONS OF CACGS

Blood Density (ρ)	1055.0 Kg/m^3		
Blood Viscosity (ν)	3.5x10^{-6} m^2/s		
Reynolds Number (Re)	89-389		
Inflow Ratio (Q_0)	60.3-263.8 ml/min		
Velocity (U)	8-35 cm/s		
	Diameter (mm)		
CACG	Native Artery	Branch-1	Branch-2
T, Y-graft	D_1=4 mm	D_2=3.8 mm	-
Sequential	D_1=4 mm	D_2=3.8 mm	D_3=3.8 mm
Π-graft	D_1=4 mm	D_2=3.8 mm	D_3=3.52 mm

equation for a compressible fluid is consisted of the four terms, namely local and convective acceleration, pressure gradient and diffusive term. The three-dimensional generalized equations are shown in equation (3) and obtained after mathematical manipulations from their Cartesian counterparts.

$$\underbrace{J\rho\frac{\partial(\vec{u})}{dt}}_{\text{Local Acceleration}}+\underbrace{\vec{u}\left(\vec{\nabla}\cdot\left(\vec{u}\cdot\vec{e}^{\,i}\right)\right)}_{\text{Convective Acceleration}}=-\underbrace{p\cdot\vec{e}^{\,\xi}}_{\text{Pressure Gradient}}+\underbrace{J\Gamma\left(\nabla\cdot\left(\vec{e}^{\,\xi}\cdot\vec{e}^{\,i}\right)\right)}_{\text{Diffusion}} \qquad (3)$$

where J is the determinant of the Jacobian, $\vec{e}^{\,\xi}$ is the reciprocal base vector in ξ-coordinate and $\vec{e}^{\,i}$ denotes the reciprocal base vectors where i = ξ, η, ζ [9]. The inner product $\vec{u}\cdot\vec{e}^{\,i}$ corresponds to the contravariant velocities (U, V, W) for three-dimensional coordinates in the transformed space shown in equation (4) [10].

$$U=\vec{u}\cdot\vec{e}^{\,\xi} \qquad V=\vec{u}\cdot\vec{e}^{\,\eta} \qquad W=\vec{u}\cdot\vec{e}^{\,\zeta} \qquad (4)$$

Geometrically, the contravariant velocities, U, V, W, signify the projection of the velocity vector $\vec{u}$ over the reciprocal base vectors $\vec{e}^{\,\xi},\vec{e}^{\,\eta},\vec{e}^{\,\zeta}$, respectively.

An arbitrary vector **A**, it can be defined with respect to reciprocal base as in (5).

$$A=A_\xi\vec{e}^{\,\xi}+A_\eta\vec{e}^{\,\eta}+A_\zeta\vec{e}^{\,\zeta} \qquad (5)$$

where A_ξ, A_η and A_ζ are the coefficients of the expansion with respect to reciprocal base vectors. The transformation or mapping of physical plane to the transformed plane is

mathematically obtained by using the Jacobian (J) and the metric tensors [11]. An illustration of the coordinates transformation in two-dimensions, for the sake of simplicity, is given in Figure 2.

The numerical solution of these equations is obtained by

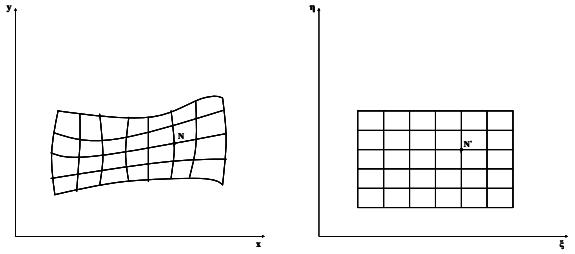

Figure 2: Arbitrary computational domains depict the mapping (transformation) from the physical plane (x, y) to the transformed plane (ξ, η) in two-dimensional space.

implementing the iterative "guess-and-correct" procedure of Patankar and Spalding [12], employing a modified version of the semi-implicit method for pressure-linked equations (SIMPLEST) algorithm. More details regarding this iterative-solution algorithm can be found elsewhere [13]-[14].

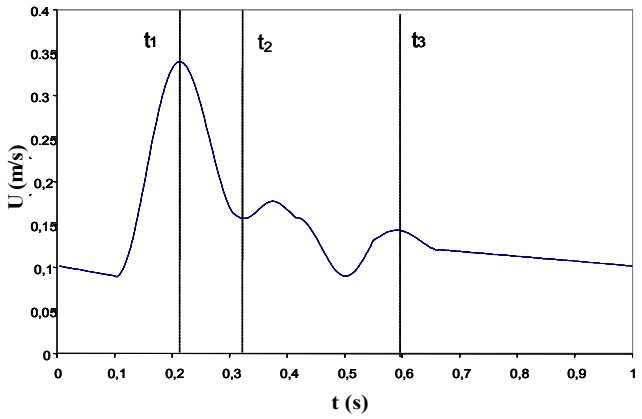

Fig.3 Physiologically realistic pulsatile inflow waveform. Three different phases are seen in the Figure, the peak systolic (t_1), end systolic (t_2) and peak diastolic phase (t_3).

C. *Boundary Conditions*

The blood is considered as Newtonian with constant kinematic viscosity of 3.5 x 10^{-6} m/s^2 and incompressible with fluid density of 1055 kg/m^3. This assumption is validly taken for medium of large vessel arteries with shear rates above 100 s^{-1}. Even though, the non-Newtonian nature significantly influences the WSS distribution in low velocity fields, a study by Johnston et al., 2006 concerning four different arteries with diameters ranging between 3 and 7 mm showed that for more than 70% of the pulse cycle the differences between Newtonian and non-Newtonian constitutive models are insignificant. In this study, both steady and unsteady flow conditions are analyzed. In the latter, the blood inflow waveform is considered pulsatile with Womersley number (α) of 2.75. This value for α ensures that the local acceleration (unsteady inertia term in momentum equation) becomes important in performing solution of flow

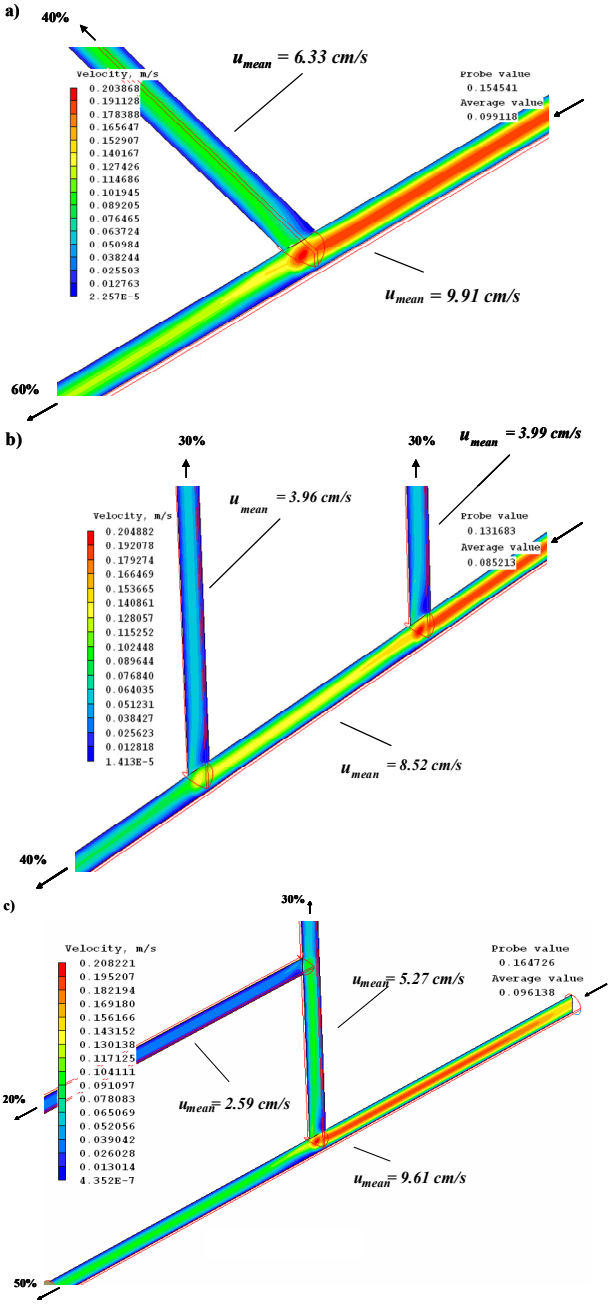

Figure 4: Velocity contours within different CACGs for steady flow conditions, a) Y-graft, b) Sequential graft and c) Π-graft. The inlet Reynolds number is 111 corresponds to mid-range velocity of 10 cm/s

governing equations.

The inflow rate for the tube diameter considered herein ranges from 60.3 to 263.8 ml/min. At outlets known pressures are assessing to assure predefined distribution of outflow rates (see Fig.1).

III. RESULTS

The computations are conducted in four geometries (see Fig.1) representing simplified versions of CACGs. For steady state simulations, various inlet velocities corresponding to Reynolds numbers ranging from 55 to 444 are imposed, while at outlets known pressures are specified in order to control outflow rate distributions. Unsteady flow simulations comprise physiologically realistic inflow waveform at inlets of the composite grafts.

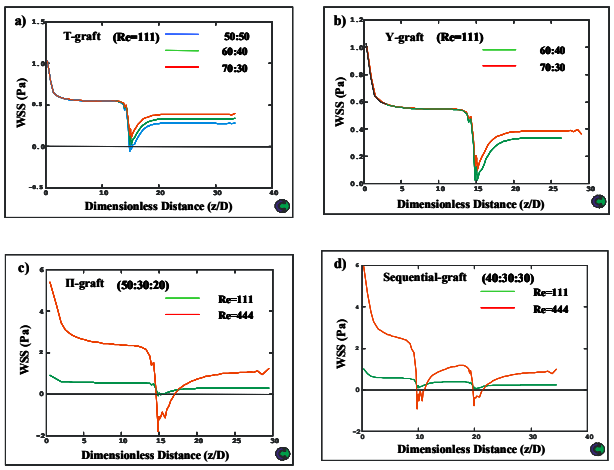

Figure 5: WSS distributions along the low wall of the native coronary artery for a) T-graft, b) Y-graft, c) Π-graft and d) Sequential graft.

A. Steady State Simulations

The steady state simulations comprise four different geometric configurations with various Reynold numbers at inlet range from 55 to 444 corresponding to inlet velocities of 5 to 40 cm/s, respectively. In Fig. 4, the distribution of velocity contours within the CACGs is shown. Proximal to the bifurcation, a parabolic velocity profile is developed with maximum velocity to be located in the centre of the vessel. In the vicinity of anastomoses the fluid flow is highly disturbed causes shifting of the bloodstream towards the heel of the vascular walls. Low velocities (dark colored regions in Fig. 4) are observed on the side walls at the turn of fluid stream and on the walls just opposite of the flow division.

TABLE 2
MEAN FLOW VELOCITIES IN CACGS

CACG	T-graft (cm/s)			Y-graft (cm/s)		
	50:50	60:40	70:30	50:50	60:40	70:30
NCA	9.19	9.99	10.62	9.12	9.91	10.87
B-1	6.51	5.23	3.95	7.28	6.33	4.77
CACG	Sequential Graft (40:30:30) (cm/s)			Π-graft (50:30:20) (cm/s)		
	Re = 111		Re = 444	Re = 111		Re = 444
NCA	8.52		32.33	9.61		36.47
B-1	5.99		15.30	5.27		19.48
B-2	3.96		15.22	2.59		10.19

Mean flow velocities within different geometries of CACGs are shown in cm/s. In single-branched geometries, three different cases, concerning various flow rate distributions are illustrated, while for double-branched geometries, two different case with inlet Re = 111 and Re = 444 are shown. The abbreviation NA denotes Native Coronary Artery, while B-1 and B-2 indicate Branch-1 and Branch-2, respectively

For single-branched CACGs (T and Y), the mean velocity within the native coronary artery takes similar values, while within the branch-1 the mean velocity is calculated with an almost 20% difference. A very low mean velocity is observed in the branch-2 of Π-graft. In Table 2, the mean velocities for different outflow rate distributions are depicted.

In Figure 5, the WSS distributions along the native coronary artery of different CACGs are shown. Proximal to the flow divider, no differences in WSS are observed for single-branched composite grafts. On the contrary, the WSS distribution takes significantly different values at anastomotic and distal to the vessel sites as shown in Figs. 5a-b. Considerably different WSSs are computed in double-branched geometries for different Reynolds numbers as shown in Figs. 5c-d. For mid-range velocities (Re=111), a smooth WSS distribution is observed, while a highly non-uniform variation of WSSs is calculated for high-range velocity values (Re=444).

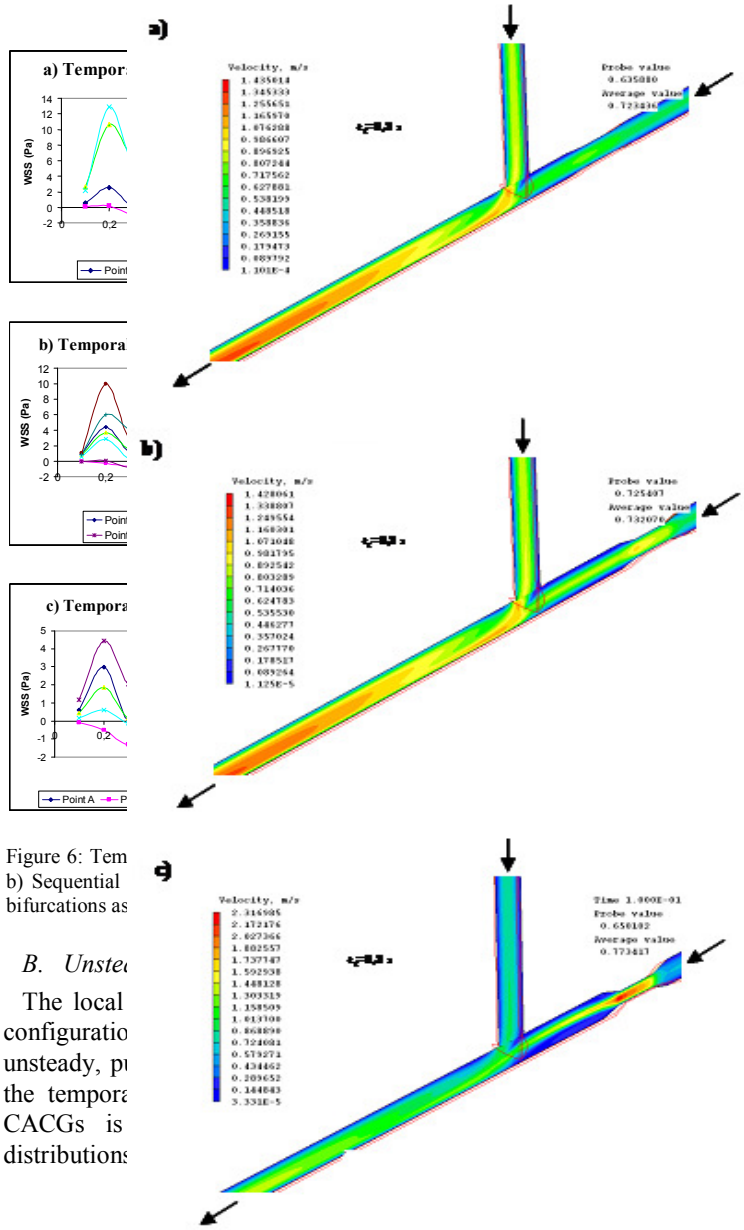

Figure 6: Tem
b) Sequential
bifurcations as

B. Unste

The local
configuratio
unsteady, pu
the tempora
CACGs is
distributions

Figure 8: Velocity contours for T-graft under different percents of native artery constrictions a) 25% , b) 50% and c) 75%. Such results refer to peak systolic phase (t=0.3s)

to bifurcations (Points A and D for Sequential geometry), the lowest WSSs are observed at end systolic phase where flow deceleration occurs. Just after flow division (Points B and E for sequential geometry) negative and/or almost zero WSSs are calculated throughout the cardiac cycle for the low vascular walls. On the upper vascular walls of native coronary artery (Points C for T and Sequential grafts) remarkably high wall shear stresses are computed showing that the bloodstream undergoes acceleration once hits on the wall heel. Likewise, high WSS are also predicted at side branches where the flow stream is directed, e.g. Point D in T-graft, Points F and G in Sequential and Point G in Π-graft.

In Fig. 7, the velocity contours in T-graft configuration for different time instances of cardiac cycle are shown. During peak systole (t_1), a fluid acceleration is occurred, while the fluid is decelerated at diastolic phase (t_2 and t_3). Due to bifurcation, the maximum velocity is shifted from the centre of vessel (prior to flow division) to the wall heel as shown in Fig.7. The flow disturbance at the anastomoses causes a stagnant fluid behavior downstream to the bifurcation. A flow recovery is observed at almost 5-8 diameters downstream to the flow divider. The maximum velocity at peak systole (t_1) is computed at 1.24 m/s, 0.8 m/s for end systole (t_2) and 0.56 m/s at peak diastole (t_3).

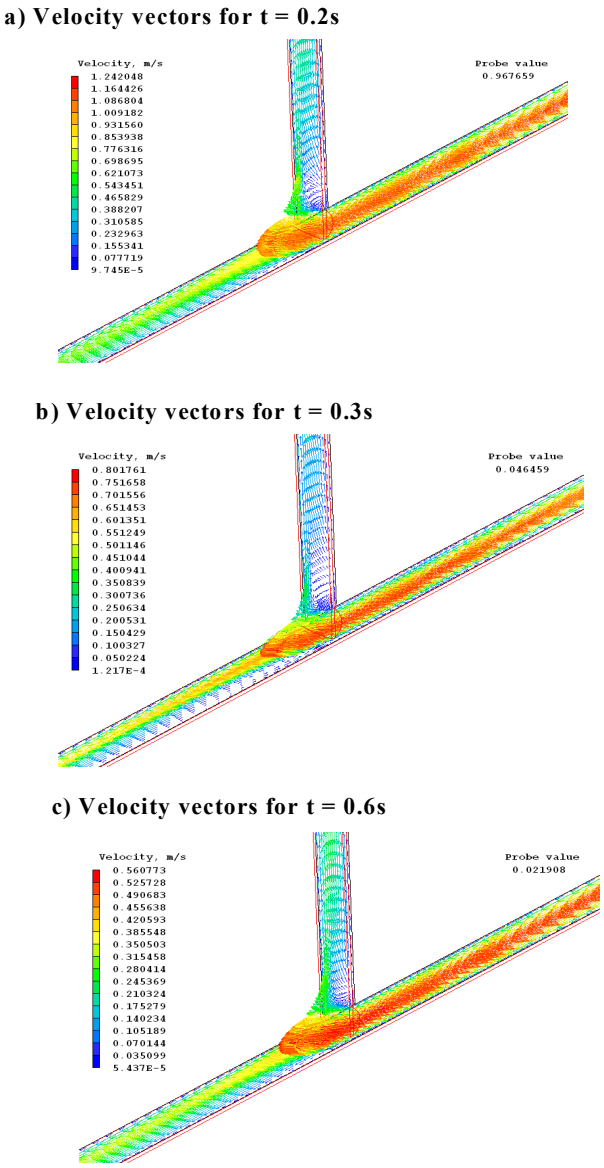

Figure 7: Velocity vectors for T-graft configurations for different time instances, a) Peak systolic phase, b) End systolic phase and c) Peak diastolic phase.

The computer simulations of pathological cases with different degrees of native coronary artery stenosis, namely 25-75%, are shown in Figure 8. In case of mid (25%) stenosis (Fig. 8a), the flow is not significantly disturbed prior to bifurcation, while for 50% constriction a zone of separation flow is developed in the vicinity of stenosis (Fig. 8b). Finally, for the severe case of lumen constriction, the fluid acceleration, due to stenosis, causes high disturbances to downstream flow. The latter is characterized by extended regions of fluid recirculation and stagnant flow behavior (Fig. 8c).

IV. Discusssion

It is well conceded that local haemodynamics strongly influenced the localization of CAD [15]. Low and/or high WSS regions, high pressure gradients along the arterial vessels and high residence time of blood cells and lipoids in specific regions within coronary system are the main risk factors for the development of CAD [9]. According to the anatomy of coronaries the most prone locations for the development of atherosclerotic lesions involve geometric configurations such as curvatures, bifurcations and branchings, resulting to large flow disturbances [16]. Additionally, in vivo models have shown that the most vulnerable places are the heel, the toe and the suture line of anastomoses and the wall opposite to the junction. Numerous computational [17]-[18] and experimental studies [19]-[20] have shown that local blood flow characteristics and WSS distribution are strongly affected by arterial geometry. Even though the appearance of low and oscillating shear stress is associated with the intimal thickening, the detailed mechanisms contribute to the progression of the disease are still unknown. Therefore, further studies are required to determine the correlation between the blood flow characteristics and CAD.

The presented simulation work concludes the followings:

1. Geometry of CACGs strongly affects myocardial blood flow especially in exercise conditions (coronary flow reserve).
2. Dealing with haemodynamics of CACGs, Π-graft is considered as the worst case while Y-graft exhibits the best flow behavior. Especialy, at branch-2 of Π-graft low velocities and WSSs are calculated indicating sites prone to flow pathologies.
3. Sites prevalent to CAD are characterized by pathological flow phenomena. These sites are found at distinct regions such as, heel, toe, the wall just opposite the bifurcations, at the turn of arterial grafts and at the lateral walls of side branches

4. Low WSS regions are associated with initiation and development of atherogenesis, while high WSSs are correlated with the damage of endothelium.
5. The case of severe pathological conditions (>75% stenosis) is accompanied with high flow disturbances able to significantly promote the development of CAD.

The future work includes the development of an experimental rig in which the test section is constructed by Plexiglas and glass. The following step is to perform in vivo experiments using pigs as animal model. Finally, this work will be extended to clinical observations on humans by employing double blind randomized prospective studies.

REFERENCES

[1] F.D. Loop, B.E. Lytle, D.M. Cosgrove, R.W. Stewart, M. Goormastic, G.W. Williams, L.A. Golding, C.C. Gill, P.C Taylor, W.C. Sheldon and W. Proudfit. "Influence of the internal-mammary-artery graft on 10-year survival and other cardiac events," *N Engl J Med*, vol. 314, 1986, pp. 1-6.

[2] B.W. Lytle, E.H. Blackstone, F.D. Loop, P.L. Houghtaling, J.H. Arnold, R. Ahkrass, P.M. McCarthy and D.M. Cosgrove, "Two internal thoracic artery grafts are better than one," *J Thorac Cardiovasc Surg*, vol. 117, 1999, pp.855-872

[3] T. Fukui, S. Takanashi, Y. Hosoda and S. Suehiro, "Total arterial myocardial revascularization using composite and sequential grafting with the off-pump technique," *Ann Thorac Surg*, vol. 80, 2005, pp. 579–585.

[4] A.N. Calafiore, G. Di Giammarco, N. Luciani, N. Maddestra, E. Di Nardo and R. Angelici, "Composite arterial conduits for a wider arterial myocardial revascularization," *Ann Thorac Surg*, vol. 58, 1994, pp. 185-190.

[5] G. Sakaguchi, E. Tadamura, M. Ohnaka, K. Tambara, K. Nishimura and M. Komeda, "Composite arterial Y graft has less coronary flow reserve than independent grafts," *Ann Thorac Surg*, vol. 74, 2002, pp. 493-496.

[6] A. K. Politis, G.P. Stavropoulos, M. N. Christolis, F.G. Panagopoulos, N.S. Vlachos and N.C. Markatos, "Numerical modeling of simulated blood flow in idealized composite arterial coronary grafts: Steady state simulations," *J. Biomech,* vol. 40, 2007, pp. 1125-1136.

[7] A. K. Politis, G.P. Stavropoulos, M. N. Christolis, F.G. Panagopoulos, N.S. Vlachos and N.C. Markatos, "Numerical modeling of simulated blood flow in idealized composite arterial coronary grafts: Transient simulations," *J. Biomech,* vol. 41, 2008, pp. 25-39.

[8] D. Liepsch, "An introduction to biofluid mechanics – basic models and applications," *J. Biomech*, vol. 35, 2002, pp. 415-435.

[9] A.I. Borisenko and I.E. Tarapov, *Vector and Tensor Analysis with Applications*. Dover Publications Inc., New York, 1968.

[10] J. F. Tompson, Z.U.A. Warsi, and C.W. Mastin, *Numerical Grid Generation*, Elsevier, New York, 1985.

[11] C. Fletcher, *Computational Techniques for Fluid Dynamics, Vol. II*, Springer Verlag, Berlin, 1991.

[12] S.V. Patankar and D.B. Spalding, "A calculation procedure for heat, mass and momentum transfer in three-dimensional parabolic flows," *Int. J Heat Mass Trans*, vol. 15, 1972, pp. 1787-1806.

[13] N.C. Markatos, and A. Pericleous, "Laminar and turbulent natural convection in an enclosed cavity," *Int. J. Heat Mass Trans*, vol. 27, 1984, pp. 755-772.

[14] D.B. Spalding, "An introduction to viscous incompressible flow," *Int J Heat Mass Transf* , vol. 23, 1980, pp. 747.

[15] J.G. Myers, J.A. Moore, M. Ohja, K.W. Johnston and C.R. Ethier. "Factors influencing blood flow patterns in the human right coronary artery," *Ann Biomed Eng* , vol. 29, 2001, pp. 109-120.

[16] B. Berthier, R. Bouzerar, and C. Legallais, "Blood flow patterns in an anatomically realistic coronary vessel: influence of three different reconstruction methods," *J Biomech*, vol. 35, 2002, pp. 1347-1356.

[17] D.N. Ku, "Blood flow in arteries," *Ann Rev Fluid Mech* vol. 29, 1997, pp. 399-434.

[18] E.S. Weydahl, J.E. and Moore Jr., "Dynamic curvature strongly affects wall shear rates in a coronary artery bifurcation model," *J Biomech*, vol. 34, 2001, pp. 1189-1196.

[19] A.M. Imparato, A. Bracco, G.E. Kim and R. Zeff, "Intimal and neointimal fibrous proliferation causing failure of arterial reconstruction" *Surgery*, vol. 72, 1972, pp. 1007-1017.

[20] V.S. Sottiurai, J.S.T. Yao, R.C. Batson, S.L. Sue, R. Jones, and Y.A. Nakamura, "Distal anastomotic intimal hyperplasia: histopathological character and biogenesis," Ann Vasc Surg, vol. 1, 1989, pp. 26-33.